Nat Hazards (2015) 75:669–699
DOI 10.1007/s11069-014-1339-5

ORIGINAL PAPER

Community-based flood damage assessment approach for lower West Rapti River basin in Nepal under the impact of climate change

E. D. P. Perera · A. Hiroe · D. Shrestha · K. Fukami · D. B. Basnyat · S. Gautam · A. Hasegawa · T. Uenoyama · S. Tanaka

Received: 21 August 2013 / Accepted: 27 July 2014 / Published online: 8 August 2014

Abstract The West Rapti River (WRR), one of the dynamic and economically important basins of Nepal, was focused in this study to understand the impact of climate change in localized scale. The adopted methodology was a community-based field survey followed by a hydrological modeling to estimate present and future flood damages for households and agriculture. Flood disaster occurred in 2007 was simulated and discussed. High-resolution atmospheric general circulation model's precipitation outputs for emission scenario A1B were utilized with their bias corrections to obtain the precipitation patterns over lower WRR basin for Present (1979–2003) and Future (2075–2099) periods. A conceptual hydrologic model was employed to obtain the time series of daily river runoffs for the above-mentioned time durations followed by frequency analyses for probable flood discharges of 25- and 50-year return periods. Flood inundation simulations of 50-year return period events for Present and Future were carried out with the rainfall–runoff–

E. D. P. Perera (✉) · A. Hasegawa · T. Uenoyama
International Centre for Water Hazard and Risk Management (ICHARM) Under the Auspices of UNESCO, Public Works Research Institute (PWRI), 1-6 Minamihara, Tsukuba, Ibaraki 305-8516, Japan
e-mail: duminda.pradeep@gmail.com

A. Hiroe
Center for Advanced Engineering Structural Assessment and Research (CAESAR), Public Works Research Institute, Tsukuba, Ibaraki, Japan

D. Shrestha · D. B. Basnyat
Nepal Development Research Institute, Lalitpur, Kathmandu, Nepal

K. Fukami
National Institute of Land and Infrastructure Management, Tsukuba, Ibaraki, Japan

S. Gautam
Welthungerhilfe - Nepal, P.O. Box: 8130, Gairidhara Marg-288, Kathmandu, Nepal

S. Tanaka
Water Resources Research Center, Disaster Prevention Research Institute, Kyoto University, Kyoto, Japan

inundation model followed by a flood damage assessment for household and agriculture based on the inundation simulation results, and field survey data over the target area and potential flood damages were discussed. Integration of hydrological modeling and socio-economic approach to foresee potential flood damages was achieved, and the adopted damage assessment methodology was systematically explained. The total increments of household and agriculture damages due to climate change were estimated for Present as 1.80 and 1.95, and for Future, it was 2.40 and 2.27, respectively, compared to 2007 flood disaster. Future flood frequencies, intensities, and consequent damages in the area show a significant increment compared to the present situation despite limitations and uncertainties.

Keywords MRI-AGCM precipitation · Climate change · Flood hazards · Flood damage assessment · Inundation modeling

1 Introduction

Floods are the most frequent natural disaster that affect societies around the globe. Dilley et al. 2005 estimated that more than one-third of the world's land areas is flood-prone, affecting approximately 82 % of the world's population. Globally, the economic losses due to extreme weather events and flood catastrophes are severe, and if those catastrophes occur in developing countries, they become unbearable economic burdens. In the context of climate change, The probability of floods that have risk to induce damage is likely to increase as a consequence of the increase in the intensity of extreme precipitation events (i.e., >100 mm/day) (Baidya et al. 2007). A consensus has emerged that developing countries are more vulnerable to climate change than developed countries because of the predominance of agriculture in their economies, scarcity of capital for adaptation measures, their warmer baseline climates, and their heightened exposure to extreme events (Parry et al. 2001). With the increasing of extreme events' frequencies, coping capacity (mitigation and frequent preparedness) will become a serious burden to developing countries. Moreover, within a developing country, rural areas will suffer severe agriculture and household losses if they have high vulnerability and exposure to the climate change-induced water-related disasters.

Among developing countries, Nepal has been identified as a frequent disaster spot and it was ranked at 11th in the world on disaster vulnerability (Dilley et al. 2005). The major natural hazards in Nepal are floods, landslides, debris flows, droughts, snow avalanches, glazier lake outburst floods, cold waves, hot waves, and hailstorms. DWIDP (2007) estimated that annual average life losses due to floods and landslides triggered by heavy precipitation in Nepal were 600 and average property damage was 626 million NPR. If describe with percentages, floods and landslides cause 29 % of the total annual deaths and 43 % of the total loss of properties in Nepal (DWIDP 2004). The majority of Nepal's present population depends on agriculture for their subsistence, although still about 63 % of the agricultural lands are deprived of modern irrigation facilities (FAO 2004). The increased precipitation variability creates difficulties in cultivating these lands and could result in probable food scarcity for the population. Currently, about 31 % of Nepal's total population is below the poverty line and 95 % of them live in rural areas (MOF 2005). Poor people are more vulnerable to climatic extremes as well as gradual changes in climate

than the rich because they have less protection, less reserves, fewer alternatives and a lower adaptive capacity, and because they are more reliant on primary productions. WRR basin is an important river concerning its significance in water supply for agriculture, irrigation, and domestic uses to the West Terai region of Nepal. The WRR of Nepal is one of the most flood-prone rivers. Each year, floods during the monsoon season induce inundation among several villages in the lower part of WRR near the Nepal-India border. The lower WRR basin has a tropical to subtropical climate while the upper WRR has temperate climate. The period from March to May is hot and dry, June to August is hot and humid, September to October is pleasant, and November to February is cool and foggy with occasional rainfall due to westerly winds. The temperature reaches 46 °C in summer in the lower part of the basin and falls below 2 °C during winter in the upper part of the basin. The study area receives summer monsoon rainfall extending from June to September, accounting about 80 % of the total annual. The average rainfall for WRR basin is about 1,500 mm. The relative humidity fluctuates as low as about 60 % in May to above 90 % in January (Gautam and Phaiju 2013). The WRR covers approximately 6,450 km^2 of basin area and has the total population of approximately 1,046,000 (CBS 2001). It originates from the Mahabharat range in Nepal with average altitude of about 3,000 m. According to topographical profile, the basin can be broadly categorized as upper region (hilly) and lower region (Terai—plain). Springs and monsoon precipitations are the main contributors for the water budget of the river.

A Nepalese rural area located in lower WRR basin in Terai region, which has been facing frequent floods and consequent damages, was selected for the study. Bank-cutting, erosion, and sedimentation are other complex geophysical processes frequently taken place in the selected area. These processes will intensify floods and possibly make the flood disaster even worse. Although the selected area frequently encounters floods, a detailed study has not been taken place to understand flood vulnerabilities. Moreover, flood damage assessment for future anticipated flood hazards has not been studied so far, which leads the settlements to an uncertain risk. Required data for hydrological modeling were hardly found, which led to a great difficulty in the process of justification of numerical results. In most of the flood-prone areas, finding relevant data is an issue, which hinders the efforts of a sound hydrological modeling and increases uncertainties in outputs. At this end, in the present study, we tried to conduct flood predictions and assessments for possible flood damages for lower WRR basin through field survey data and integrating three models named as Japan Meteorological Research Institute-Atmospheric General Circulation Models (MRI-AGCM 3.1S and 3.2S), Parameter Distributed Hydrological Model of Public Works Research Institute (PDHM) (Inomata and Fukami 2007; Sugiura et al. 2009), and Rainfall–Runoff–Inundation (RRI) model (Sayama et al. 2011). Combining these three models, despite the uncertainties caused by the limitation of quantitative data on historical flood disasters in the target area, we were able to generate inundation information regarding possible flood hazards. Using obtained inundation distributions and field survey information, damage assessments for household and agriculture were carried out for 2007 flood event, Present and Future time periods' 50-year return period floods. Although other hydroenvironmental issues were also significant in causing floods in the selected area, in the present study, authors focused only the extreme precipitation-based floods to assess household and agricultural damages. This study did not consider the future developments for flood mitigation and prevention in the selected area. Therefore, the achieved result is thought to be even minimal scenario in the case of no action is taken place in future for flood prevention or mitigation.

It is very important and urgent matter to assess the impact of floods in rural agricultural areas and to prepare long-term plans for risk management. This will assist policy makers to

better understand the vulnerability of developing rural areas under socioeconomic and climatic changes because their agricultural contribution to the country's economy is significantly high. Studies conducted at global and regional levels provide a general overview of the situation in their respective contexts (Nicholls et al. 1999; Nicholls 2002); however, such results do not present comprehensive details to provide a sound basis for developing the best strategies for flood risk management in localized conditions as discussed in this paper. At present, a comprehensive picture of the flooding situation and its impacts is not captured at the required level for appropriate management strategies to be devised by the responsible organizations. So far, only a few studies have been conducted in this direction, and a very few Asian countries have prepared long-term plans to deal with these problems. Significant progress has been made in two-dimensional hydrological and hydrodynamic modeling in the last 10 years, and several models have been developed that are highly capable of simulating flood inundation and of assessing the socioeconomic impacts of floods (Parker 1992; Jonge et al. 1996; Dutta and Tingsanchali 2003; Brouwer and van EkR 2004; Jonkman et al. 2008). However, sufficient progress has not been made so far on integrating social science and hydrology to study the impacts of floods in rural agricultural communities under socioeconomic and climatic changes. This study aimed to develop an integrated tool to analyze the socioeconomic impacts of floods in rural areas under projected climatic conditions.

The study area is located in the lower WRR basin near the Nepal–India border, Nepalgunj in Banke district of Nepal. As shown in Fig. 1, the WRR basin consists of three river runoff stations named as Bagasoti, Julkundhi, and Kusum and several number of ground rainfall stations. The catchment areas of the basins of Bagasoti, Julkundhi, and Kusum are 3,608, 5,151, and 5,348 km^2, respectively. The study area is shown in Fig. 1, which covers both India and Nepal; however, our study focused only the Nepal. The locations of Kalkaluwa embankment and the India–Nepal border are also shown in Fig. 1. The study area faces recurrent flood disasters where significant losses of properties, lives, and livelihood of the local population occur. Recent extreme flood events in WRR were reported in 1977, 1981, 1983, 1989, 1998, 2006, 2007, 2009, and 2012. The flood occurred in 1981 was reached to 100-year return period flood (Gautam and Phaiju 2013). The recorded flood damages of 2006 flood event are shown in Table 1. On October 7, 2009, the flood discharge in WRR exceeded the danger level and reached 4,860 m^3/s. In Banke district, 2 people died, 1,456 families were displaced, and 2,683 families were affected (UN OCHA Nepal 2009). Floods are caused by both mainstream of WRR and local heavy rainfalls, contributing to high flows in the tributaries. It is reported that the inundation problem has been worsened by the construction of the Kalkaluwa embankment in Indian side near to the border, due to the obstruction of natural drains and flows from WRR (UNDP 2009). In future, anticipated climate change-induced high precipitations will be intensified flood inundations in this area. The study area was covered by six Village Development Committees (VDCs) namely Bankatti, Betahani, Gangapur, Holiya, Kamdi, and Phattepur in the lower WRR Basin as shown in Fig. 2. Those VDCs, which are explained in Table 2 and shown in Fig. 2, were categorized as most affected, moderately affected, and less affected according to the historical inundation severity based on the information received during the field surveys conducted by the authors in June 2011 and previous literature (Osti 2008). Gangapur and Holiya VDCs, which are located near to the Indian border, suffer severe losses due to frequent floods as learnt during the field survey. Agriculture-based economy prevailed in the study area, and the population was approximated as 45,000 in 2001 (CBS 2001). The land cover was mainly consisted of farmlands, forests, and villages as shown in Fig. 2.

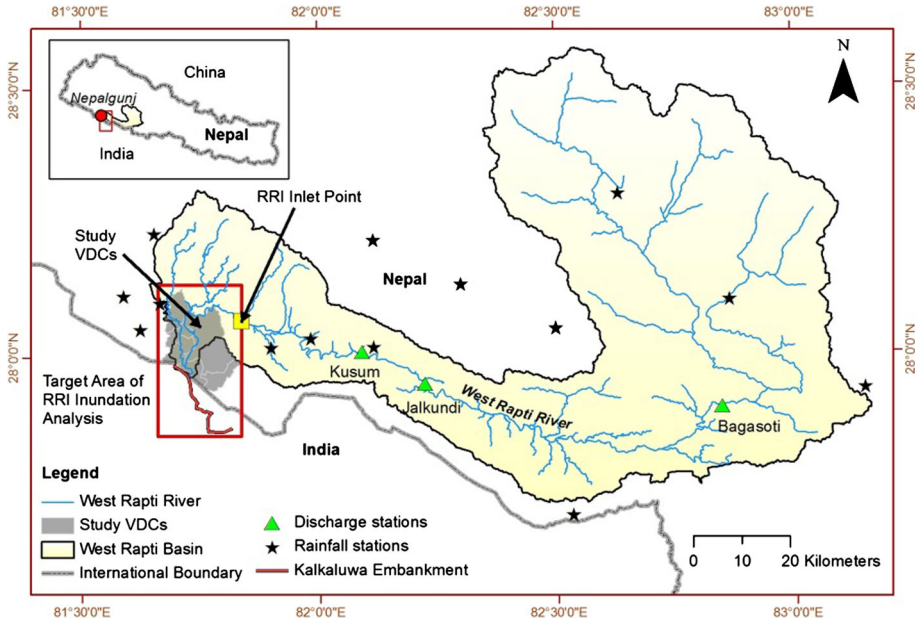

Fig. 1 Map of WRR basin, rainfall stations, discharge measuring stations, and study area

2 Methodology

2.1 Field survey

Authors conducted a field survey to assess the current socioeconomic status of the affected communities as well as to assess the exposure of household assets, properties, and agricultural crops to floods and potential loss (damage) due to different depths and durations of floods. Secondary data on agricultural production were also collected and analyzed. Focus Group Discussions (FGDs), Key Informant Interviews (KII), and detailed questionnaire survey were conducted during the field survey. These data were then analyzed to prepare the flood–damage curves concerning flood damages' relationship to flood depths and durations. To envisage the entire impacts of the floods on local people's livelihoods, the study area was selected on the basis of degree of flood impacts on local people. Categorically, high impact, moderate impact, and less impact areas were identified through discussion with local resource persons, which also included locally hired enumerators. A total of 120 households were surveyed accordingly by designing semi-structured questionnaire. Figure 2 includes the VDCs selected for household survey. The VDCs located in lower part are quite vulnerable in terms of floods, and they are categorized as mostly affected in Table 2. Likewise, the villages located in upper part are moderately vulnerable, whereas the villages located in middle part are less vulnerable in comparison with lower and upper part of the study VDCs. Table 3 shows the study area and the number of households selected to conduct the household survey and their composition. The total population of the surveyed households is 886, among which 476 (53.7 %) are males and 410 (46.3 %) are females. The average family size of the most affected areas is 7.5, which is followed by 7.4 in moderate affected areas and 7.3 in less affected areas. It is observed

Table 1 Flood damages in Banke district in the year 2006

VDC	Population affected	Household affected	Agricultural land affected (ha)	Losses due to physical damages (USD)
Matehiya	1,643	373	0.8	80,361
Gangapur	4,063	745	180.0	766,902
Holiya	5,159	1,349	639.8	1,437,097
Bethani	5,793	1,963	39.1	166,405
Phattepur	3,758	544	144.7	577,806

Source: Osti (2008)

that the families in the most affected area are low-income families with larger family sizes than other two household categories.

Table 4 reveals income sources of the respondents. It shows agriculture as the main source of living in the households of all the impact categories, which is followed by daily wages, salaried employment, business, and foreign employment are the other sources of income for the surveyed households. Agriculture and the daily wages are the best options to sustain livelihoods for most of the household in the study area as they represent 69.2 and 20.8 % contribution for the villagers' income. However, most households lack the income they needed to run the household every month.

Figure 3 shows different roof types observed in the study area. Construction materials of roofs and walls are the indicators to determine the economic and social status of the families in the area. According to Table 5, most walls of the respondents' houses were constructed either by stone/mud (44.2 %) or wood/bamboo (40.0 %), which comprise 84.2 % of the total. Respondents' houses with cemented wall contain 14.2 % and walls with asbestos sheets comprise 1.7 % of the total. Wall constructed with mud, wood, and bamboo cannot be considered as secured as cemented and stone walls. Table 6 shows that 65 % of households in most affected area have been constructed their roof with thatch/straw, which is considered as insecure during heavy rains. In contrary, 37.5 and 47.5 % households located in moderately and less affected areas have been constructed their roofs by tile/fabric. The roof type is a clear indicator of the community, which shows their income levels. Table 7 explains that most of irrigated cultivable lands are in the distance of less than 200 m from the WRR, which leads to a high vulnerability in a flood event. Totally, 63 agricultural lands own by the community located less than 200 m from the river and about 60 % of them are in most affected and moderately affected VDCs.

2.2 Modeling approach

The most widely used approach to simulate the hydrological impacts of climate change is to combine general circulation model (GCM) outputs with a deterministic hydrological model that contains physically based or conceptual mathematical descriptions of hydrological phenomena. The proposed methodology for carrying out inundation simulation and flood damage assessment for the study area is systematically explained in Fig. 4. The MRI-AGCMs' precipitation outputs, which were based on the IPCC Special Report on Emission Scenario A1B, were utilized in this study. The A1B scenario involves an intermediate emission scenario characterized by a very rapid economic growth, global population peaks in the middle of the twenty-first century and declines thereafter, and a balanced introduction of new and more efficient technologies of all energy supply (IPCC 2007). The

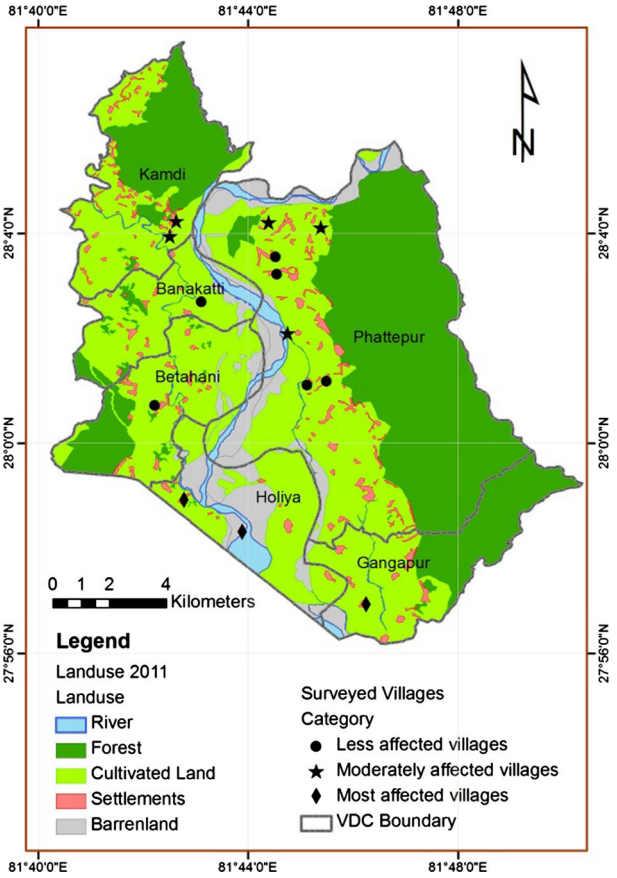

Fig. 2 Land cover, VDCs, and WRR flow path in the study area

MRI-AGCM data were made available at the institutional level for three 25-year periods such as 1979–2003, 2015–2039, and 2075–2099, termed as the Present, Near-future, and Future periods, respectively. The horizontal grid size is about 20 km in MRI-AGCM3.1S and 3.2S (Kitoh et al. 2009; Mizuta et al. 2012). While the resolution is high enough for the hydrological modeling in this region, the MRI-AGCM precipitation still has bias. Therefore, MRI-AGCM precipitation is bias-corrected without modification of horizontal resolution. According to Chen et al. 2012 in the process of studying climate change impact, the main uncertainties are from the GCMs and the downscaling sector. GCMs provide information at a resolution that is too coarse to give results that can be used directly in hydrological modeling (Vaze and Teng 2011). Hydrological model, PDHM, was used to simulate river runoff for the Present, Near-future, and Future periods based on bias-corrected MRI-AGCM precipitations. The simulated daily river discharges for the Present, Near-future, and Future were used in the flood frequency analysis using the peak over threshold (POT) method. The probable maximum flood peak discharge for 25- and 50-year return periods was obtained for the RRI model inlet point (Fig. 1). Inundations were simulated for the 50-year floods of Present and Future time periods by employing RRI model for the study area as shown in Fig. 1 and for the 2007 flood event as well. RRI inlet

Table 2 VDC categories in the study area

Degree of affectedness	Criteria	VDCs (40 households in each VDC were interviewed)
Most affected	House completely or partially collapsed, loss of lives and livestock, inundation for longer period, people suffering from waterborne diseases, flood depth up 70 cm, flood standing for more than 3 days	Gangapur, Holiya
Moderately affected	Cracking the wall of houses, falling down of wall, damage of stored food, sedimentation in the crop land, flood depth up to 30–70 cm, flood standing between 1 and 3 days	Kamdi, Phattapur
Less affected	Minor destruction, minimal damage of grain, damage of standing crops, damages of newly planted crops, flood depth less than 30 cm, flood standing for less than 1 day	Bankatti, Betahani,

point river runoff and rainfall were the hydrological stresses for inundation model. Lack of measured inundation distribution data was a limitation in validating the inundation model. However, 2007 flood event, which was the only event authors could quantify the flood disaster realities as much as possible through field survey, was simulated and compared with the VDCs categorization (Table 2) to check whether the most, moderately, and less affected village locations were correctly corresponded with the simulated inundation.

2.2.1 MRI-AGCM output precipitations and bias correction

The MRI-AGCM 3.1S provided information on possible climate change induced by global warming, including future changes in tropical cyclones, the East Asia monsoon, extreme events, and blocking anticyclones (Kitoh et al. 2009). MRI-AGCM 3.2S is the improved version with various new parameterization schemes and shows improvements in simulating heavy monthly-mean precipitation around the tropics on the Western Pacific, the seasonal pattern of the East Asian summer monsoon, and so on (Mizuta et al. 2012). The Future (2075–2099) climate experiments of MRI-AGCM 3.1S and 3.2S were called as SFOAC and SFAC, while the Present (1979–2003) climate runs were called as SPOAC and SPAC, respectively. For Near-future (2015–2039), they were called as NFOAC and NFAC. Bias correction was needed to remove the bias in the AGCM outputs. In this study, a statistical bias correction method developed by Inomata et al. (2009) was applied. The basic idea of the bias correction method was to adjust the probability distribution of GCM daily precipitation to that of its observed counterparts. Applied bias correction method was tested for Yoshino River basin, Japan, and its results showed appropriate corrections for GCM bias in both monthly and extreme daily precipitations (Inomata et al. 2009). Bias correction for the MRI-AGCM outputs was carried out considering the Asian Precipitation Highly Resolved Observational Data Integration Toward Evaluation of the water resources (APHRODITE) dataset. APHRODITE is a observational dataset of daily precipitation for the Present time period, a prototype of the gridded daily rain gauge dataset on the global land surface during 25 years between 1980 and 2004, developed in JMA/MRI succeeding to the APHRODITE project (Yatagai et al. 2009; Kamiguchi et al. 2010).

Table 3 Total population and family sizes of surveyed households

Household category	No. of households	Total	Male	Female	Average family size
Most affected	40	301	158	143	7.5
Moderate affected	40	294	162	132	7.4
Less affected	40	291	156	135	7.3
Total	120	886	476	410	7.4

Table 4 Main income sources of surveyed households

Household category	Sources									
	Agriculture		Business		Salaried employment		Daily wages		Foreign employment	
	f	%	*f*	%	*f*	%	*f*	%	*f*	%
Most affected	29	72.5	2	5.0	0	–	9	22.5	0	–
Moderate affected	24	60.0	3	7.5	4	10.0	8	20.0	1	2.5
Less affected	30	75.0	0	–	2	5.0	8	20.0	0	–
Total	83	69.2	5	4.2	6	5.0	25	20.8	1	0.8

f frequency

2.2.2 *PDHM: river runoff simulation*

The PDHM is a conceptual model with three tanks to represent surface flow (surface tank), groundwater flow (lower tank), and river discharge (river course tank). The simultaneous flow exchange between tanks is controlled by various parameters. The distributed nature of tanks within the model area gives freedom to consider various land uses as well. PDHM model with 800 m × 800 m resolution and simulation time interval as 1 day was calibrated for the river discharge data for 2006 and 2008 at two river discharge gauges (Bagasothi and Julkundi: Fig. 1) where the simulation was based on measured rainfall data obtained from rainfall stations. Seven flood events in 2006 and 2008, which had peak discharges above 1,000 m^3/s at Kusum station, were selected for the calibration. PDHM model's parameters were tuned by trial-and-error method to achieve the differences between observations and simulations minimum for seven flood events at Bagasothi and Julkundi river gauging stations. Figure 5 shows comparisons of observed and PDHM model results for Bagasothi and Julkundhi measuring points where the river discharge calculate was based on bias-corrected MRI-AGCM 3.1S and 3.2S precipitation data of 20 km × 20 km mash for time period from 1980 to 2005. Table 8 shows the error estimations for simulation results. According to Table 8, the simulated discharges at hydrological stations and their measurements are in relatively good agreements. The coefficient of determination (CD), relative root mean square error (RRMSE), linear regression coefficient (R^2), and Nash–Sutcliffe efficiency (E) were used to evaluate the predictive accuracy of the model. Considered error indicators showed reasonable estimates, which implies that PDHM model was good in performances and applicable in carrying out hydrologic modeling to predict future runoff. Calibrated PDHM model was used to generate river discharges at RRI model inlet point (As shown in Fig. 1) where those discharges were used as one of the input stress to inundation simulation model.

Fig. 3 Household types in the study area according to the roof type: **a** cement, **b** tile/thatched, **c** thatched, **d** asbestos, **e** GI sheets

Table 5 Wall types of surveyed households

Household category	House wall types							
	Cement		Stone/mud		Asbestos sheets		Wood/bamboo	
	f	%	*f*	%	*f*	%	*f*	%
Most affected	5	12.5	9	22.5	1	2.5	25	62.5
Moderate affected	8	20.0	14	35.0	1	2.5	17	42.5
Less affected	4	10.0	30	75.0	0	0.0	6	15.0
Total	17	14.2	53	44.2	2	1.7	48	40.0

f frequency

Table 6 Roof types of surveyed households

Household category	Type of roofs							
	Cement		Tile/fabric		Asbestos		Thatch/straw	
	f	%	*f*	%	*f*	%	*f*	%
Most affected	7	17.5	3	7.5	4	10.0	26	65.0
Moderate affected	8	20.0	15	37.5	5	12.5	12	30.0
Less affected	5	12.5	19	47.5	6	15.0	10	25.0
Total	20	16.7	37	30.8	15	12.5	48	40.0

f frequency

Table 7 Distance to agriculture lands from WRR (km)

Household category	$d \leq 0.2$	$0.2 < d \leq 0.5$	$0.5 < d \leq 1.0$	$1.0 < d \leq 1.5$	$1.5 < d \leq 2.0$	$d > 2.0$	Total
Most affected	23	5	2	0	0	1	31
Moderate affected	16	0	3	2	0	0	21
Less affected	24	3	3	0	1	1	32
Total	63	8	8	2	1	2	84

d distance

2.2.3 *RRI model: inundation simulation*

The RRI model simulates the processes of rainfall–runoff–inundation simultaneously based on two-dimensional diffusion wave equations (Sayama et al. 2011). The model equations are derived based on mass balance equation and momentum equation for gradually varied unsteady flow. Topographical data, flow directions, and flow accumulations, which were required for the model development, were obtained from HydroSHEDS (3-s resolution: 90 m × 90 m) (Lehner et al. 2008). For the river cross sections, 500 m width and 1.0 m depth constant cross section was selected considering the available field measurements. RRI model was employed to simulate the inundations for 2007 flood event

and 50-year return period floods of SPAC and SFAC events. River runoff generated by PHDM model for the RRI inlet (Fig. 1) and relevant rainfalls were the hydrological stresses for the RRI model to generate inundations for the selected area. The Kalkaluwa embankment, which blocks the flows of natural drains and prevents the spillover of WRR flood across the right bank of the river and thus inundates villages in Nepalese side, was also incorporated in the RRI model due to its significant impact to the community. However, the Laxmanpur barrage, which is located further downstream of the selected study area, was not considered in the inundation simulations assuming that its capacity would not be large enough to capture extreme river discharges as considered in inundation simulations. Similarly, the impact of Sikta irrigation project lies upstream to the study area was not considered in the present study. The intake head regulator for this irrigation scheme is designed for the maximum diversion capacity of 62.5 m^3/s, and the project diverting water by a run-of-river diversion structure is not designed for flood control (DOI 2014). Since our flood analysis is based on the discharge above threshold level (1,500 m^3/s), the effect of irrigation scheme on flood considered is very small.

3 Results and discussion

3.1 2007 Flood event

The selected area suffered a severe flood disaster in 2007. The rainfall data of the monsoon period (June–September 2007) of three stations namely Dang, Kusum, and Nepalgunj, which are located in the lower WRR basin, are shown in Table 9. The table shows that the rainfall was quite high in the area from July to September especially the Nepalgunj station. The total monsoon rainfall in 2007 was about 180 % higher than the normal monsoon rainfall in the station. As shown in Table 9, other two rain gauge stations also show higher rainfall particularly in the month of July. Bethani, Holiya, Pettepur, Matehiya, and Gengapur were most affected VDCs in the area by 2007 flood. In Gangapur, inundation level raised up to 1 m and the area was flooded for 3–4 days. During the flood, three houses were completely collapsed and 25 tons of paddies were totally lost. Residents were affected by waterborne diseases such as diarrhea and dysentery. Large number of livestock suffered death due to floods.

Figure 6 shows flood discharge hydrograph at RRI boundary, which was obtained from the calibrated PDHM model and the observed rain fall. There were 3 rainfall stations in the inundation model domain, and their measured rainfalls were considered for the inundation model with the boundary discharge of calibrated PDHM model. According to the flood hydrograph, the maximum discharge at the boundary was approximately 1,950 m^3/s. During that time, the maximum rainfall had recorded as 190 mm/day. Inundation distributions and depths were obtained for VDCs of the selected area, and flood hazard maps were prepared for 2007 flood event. Direct validation of the inundation results was not possible due to the lack of measured data related to the inundation depths and distribution. The VDCs located near to the Nepal–India border were severely flooded according to the field survey information, and the inundation simulation also shows a similar trend. Figure 7 depicts the inundation development at villages during 2007 flood. The simulated flood distribution for 2007 flood and its depths shows similarity with the VDC categorization as shown in Fig. 2. Simulated flood depths as shown in Fig. 8 in Piprahawa and Chaupheri show high values, and those results correspond well with VDC categorization since those villages were located in most affected area. According to the field survey data, the flood

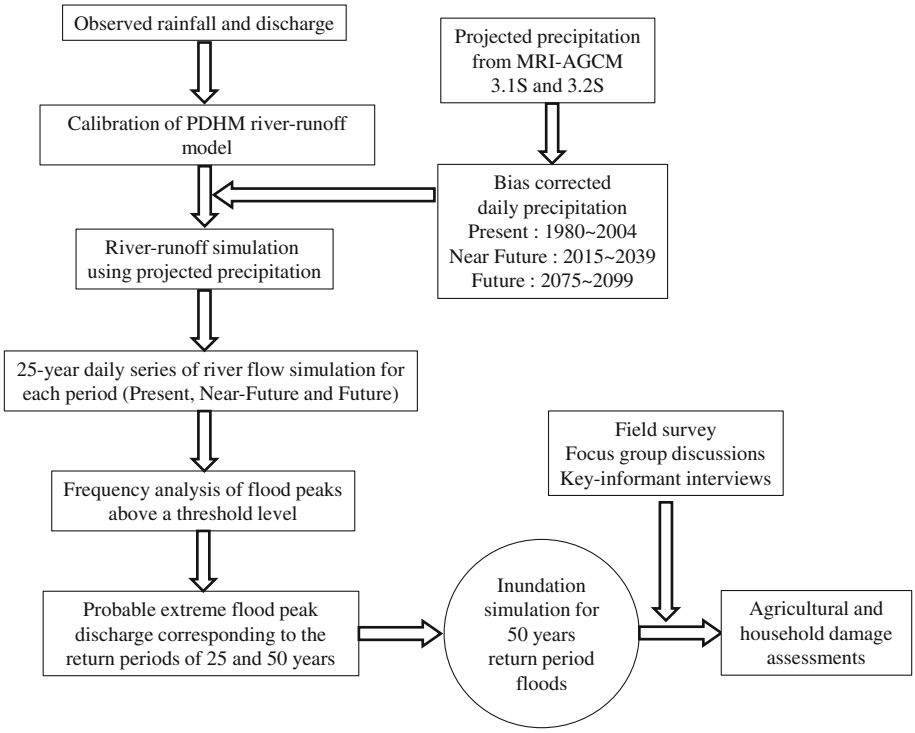

Fig. 4 Flowchart for the adopted hydrological modeling methodology for flood damage assessment

depth above 0.3 m causes significant damages to the agriculture especially for the paddy if the plants are at initial stage. According to the Figs. 7 and 8, it can been noticed that the inundation depths follow the rainfall pattern closely, which means that in this area, the floods are due to not only high river discharges, but also from the rainfall and surface runoff. The main reason for such kind of inundation distribution is the plain topography in the area.

3.2 Future inundation simulations

Figure 9 shows RRI inlet discharges that were simulated by PDHM model based on the bias-corrected MRI-AGCM 3.2S outputs. It can be seen that the river discharge at the RRI inlet point has increased twice from Present (SPAC) to Near-Future (SNAC) and Future (SFAC). An overall increment of discharges can be seen compared to the Present time period. In SPAC, the peaks have occurred in June or July most of the times; however, for SNAC and SFAC, the appearances of high peaks have been shifted to September and October. In SPAC, the peak events' discharges were less than 4,000 m^3/s; however, in SNAC and SFAC, the frequencies of peaks above 4,000 m^3/s are significantly high. According to the methodology shown in Fig. 4, the frequency analyses were carried out for the 25-year sets of river runoff results of the RRI inlet point using peak over threshold (POT) method to obtain the 25- and 50-year return period river runoff discharges. The primary objective of frequency analysis is to relate the magnitude of extreme events to

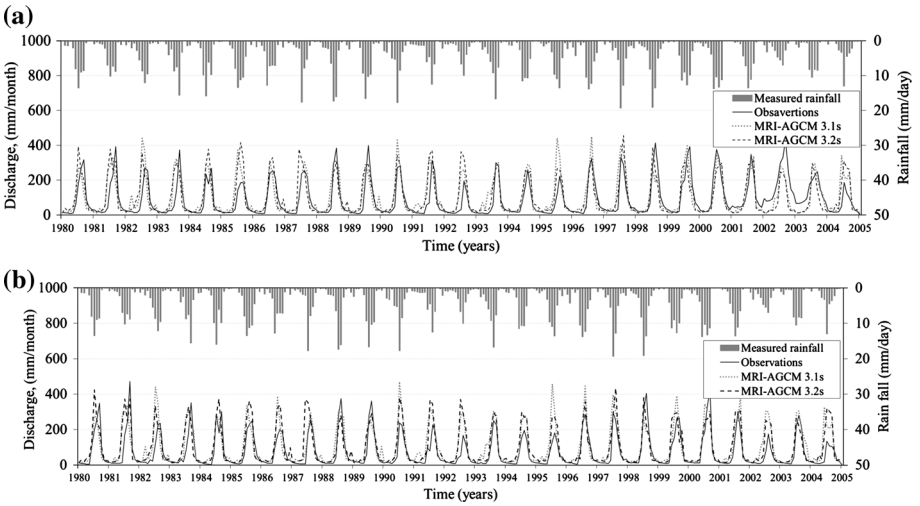

Fig. 5 Comparison of simulated and measured discharges at **a** Bagasothi and **b** Julkundi. River runoff results are based on MRI-AGCM 3.1 and 3.2 s rainfall inputs. The observed river discharges and rainfalls are also shown

their frequency of occurrence through the use of probability distributions (Chow et al. 1988). The return periods were obtained by fitting the river runoff values to Gumble distribution. Table 10 shows the results of return period calculation and frequency analysis. Frequency of occurrence of flood discharges more than 1,500 m^3/s in SFAC has increased by 2.2 times compared to SPAC. Similarly, the discharges for 25- and 50-year quantiles have been increased close to two times. These results show the possible Future climate changes compared to Present situation. Probable peak discharges increase remarkably in Near-Future, and they increase slightly at the end of twenty-first century for MRI-AGCM 3.2S. Frequency of flood increases in Near-Future and Future. 25- and 50-year peak discharges, which were calculated based on PDHM output discharges under the observed rainfalls, have the values of 3,910 and 4,350 m^3/s, respectively. The 50-year return period flood of MRI-AGCM 3.2S is more than double of the peak discharge value based on observed rainfalls. According to the obtained results, it is found that MRI-AGCM 3.2S shows extreme return period discharges than MRI-AGCM 3.1S. 50-year return period river runoff of MRI-AGCM 3.2S shows the highest value of 8,806 m^3/s among all other return period discharge values.

The inundation simulations for Present and Future 50-year return period flood events for MRI-AGCM 3.2S are discussed, and damage assessments for 2007 flood, Present (SPAC), and Future (SFAC) are elaborated in next section. According to Table 10 for 50-year return period floods, for Present, SPAC shows the highest value and for Future, SFAC shows highest value. SNAC value for 50-year return period flood is close to SFAC value. Therefore, SNAC was not considered for inundation simulation.

The inundation analysis for 50-year return periods of Present (SPAC) and Future (SFAC) was carried out based on rainfall and river discharge as shown in Figs. 10 and 12, respectively. RRI simulation results of inundation developments for each case are elaborated in Figs. 11 and 13. Comparing Figs. 11 and 13, it can be identified as the severity of extreme flood hazards. The VDCs, especially located near the Nepal–India border, will

Table 8 Statistical indices for monthly average discharge

Statistical indices	Bagasothi		Julkundhi	
	MRI-AGCM 3.1S	MRI-AGCM 3.2S	MRI-AGCM 3.1S	MRI-AGCM 3.2S
N–S efficiency coefficient (E)	0.44	0.50	0.37	0.43
Coefficient of determination (CD)	0.80	0.78	0.68	0.68
Relative root mean square error (RRMSE)	0.91	0.87	1.02	0.97
Linear regression coefficient (R^2)	0.59	0.63	0.61	0.65

highly be affected according to the obtained results. In Table 11, the inundation areas, which exceed the 30-cm flood depth, are shown with ratios comparing with 2007 flood disaster. Increment ratios of 1.8 and 2.2 are obtained for the inundation areas of above 30 cm for SPAC and SFAC cases, which shows the severity of Future floods in the study area. In 2007, the peak discharge was about 2,000 m^3/s; in SPAC, it was 4,660 m^3/s; and for SFAC, it was 8,810 m^3/s. The inundation distributions for above-mentioned flood peaks show their impacts to the target area. In the target area, when the flood depth exceeds 30 cm, the property and agricultural damages are high according to the field survey due to the plain topographic feature of the area. It is noticed that in Future, the inundation area exceeding 30 cm will be doubled compared to 2007 flood. A possible reason for the high flood levels in Holiya VDC can be explained as due to the Kalkaluwa embankment had been constructed nearby Nepal–India border. The Nepal–India border and the location of Kalkaluwa embankment are shown in Figs. 11 and 13 as well. The embankment was constructed very near to the border, and it was identified that this construction was one of the cause of inundation especially in Holiya during the field survey and also it was concerned at the time of 2007 flood. However, to understand the behavior of this embankment in a flood event, a very detailed simulation study should be carried out. When the flood discharge becomes higher, the VDCs, which were classified as less or moderately affected, are also showing high levels of floods, which has potential to lead severe disasters in Future. Consequently, there will be more damages to human lives and properties in the area if adaptation and mitigation measures are not taken in time.

Table 12 compares Present and Future inundation characteristics for MRI-AGCM 3.2S. The increment ratios for all features shown in Table 12 are greater than 1, especially the frequency of discharge exceeding 1,500 m^3/s shows the highest increment of 2.2, while the increment ratios for the frequency of precipitation exceeding 50 mm/day and 1/50 peak discharge also show significant increments according to Table 12. All these indicators illustrate the seriousness of Future flood vulnerability in the area.

3.3 Flood damage assessment for 2007, Present (SPAC), and Future (SFAC) flood events

Flood damage assessment was carried out by combining inundation results with exposure and vulnerability data. A household level socioeconomic survey, FGDs and KII were conducted in the six VDCs to assess the socioeconomic status/vulnerability of the local communities and to assess the damages faced by the communities in previous events. These data were then analyzed to prepare flood–damage functions/curves for household

Table 9 Rainfall of Dang, Kusum, and Nepalgunj stations in 2007 monsoon period

Station	Month	Total rainfall (mm)	% of monthly normal
Nepalgunj	June	181.9	84
	July	1,083.9	235.3
	August	698.2	213.1
	September	351.8	173.5
Dang	June	282	104.4
	July	645.6	166.3
	August	417.7	95.9
	September	194.3	78.3
Kusum	June	167.7	86.5
	July	903.2	256.4
	August	267.9	82.6
	September	212.3	83.3

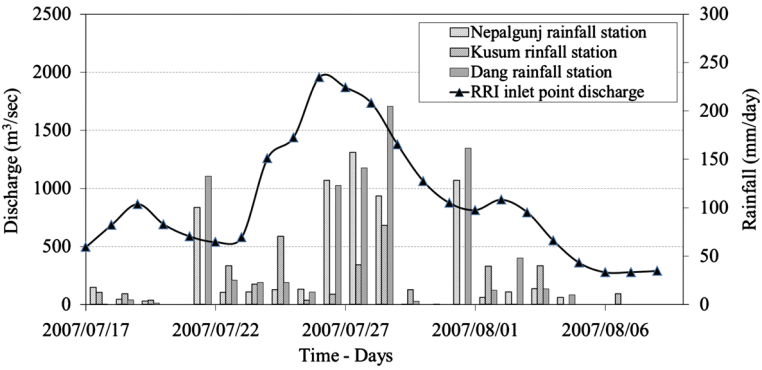

Fig. 6 Flood hydrograph for 2007 flood event at RRI inlet point and rainfalls of three stations in the study area

and agricultural damages. Agricultural damages considered in the study focused only the paddy that was cultivated in the area during the flood season. The percentage of damage to paddy grown in the area was estimated through FGDs and KIIs and verified with local experts. The damage functions and their spatial variation in the study area were then combined with the simulated inundation maps to conduct a monetary assessment assuming no change in household density/value and land cover in the area between Present and Future time intervals. In this study, socioeconomic impact of flood is defined as the potential damages from a flood event, derived by assessing the vulnerability of households and main agriculture in the area, paddy, to flood hazards. The lack of a globally accepted methodology to assess the socioeconomic impacts of floods has greatly limited the capacity to figure out a comprehensive picture in this study. The present assessment method relies on the number of households, their socioeconomic conditions, and agriculture activities of the study area. Other social and economic issues affected by the floods were not considered in the study due to the lack of sufficient data to establish a sound damage assessment. The

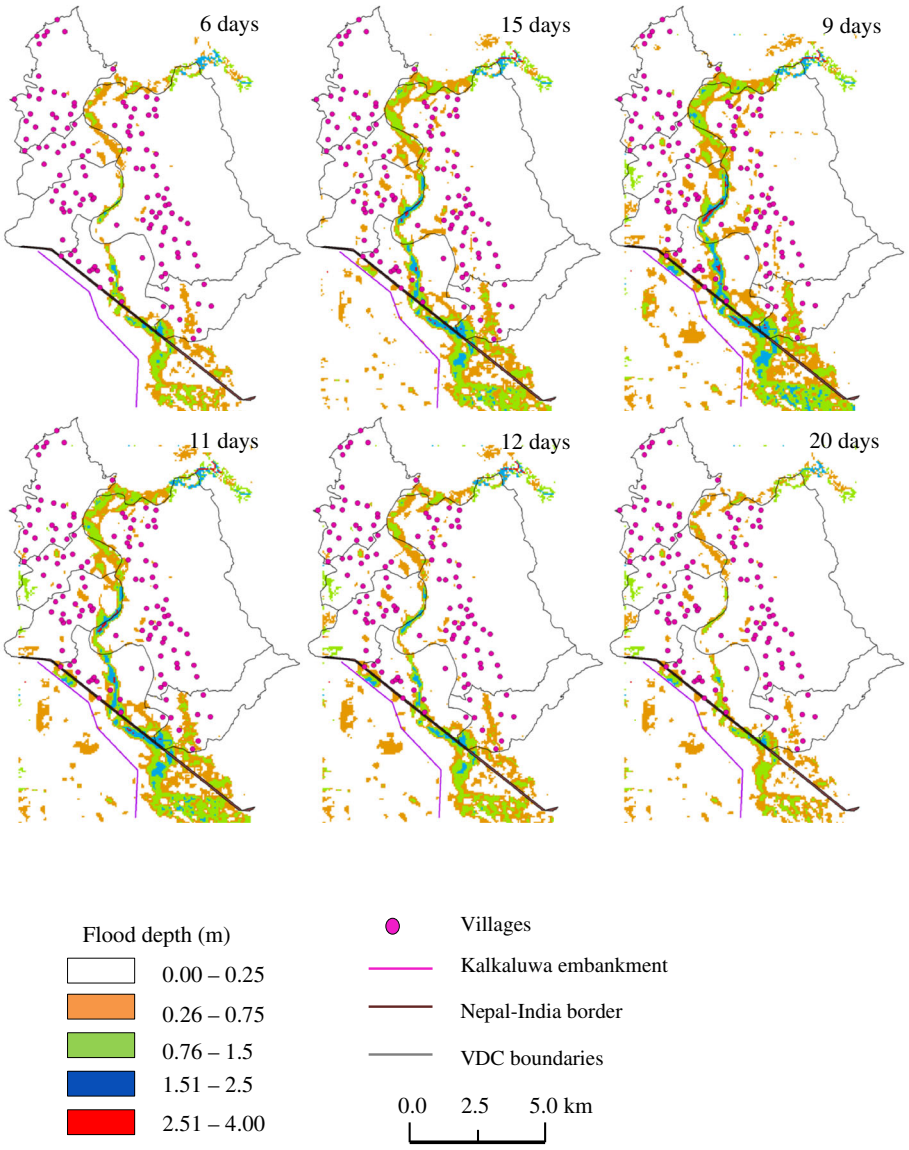

Fig. 7 Simulated inundation propagation for 2007 flood event

approach adopted to assess household and agriculture damages assumed population, land cover, household distribution, and monetary values were stationary for Present and Future though the reality is likely to vary due to several reasons such as variations in population, household density, land use, flood protection, and mitigation activities. The damages were evaluated in Nepal Rupees, and for Future, inflation of Nepal Rupee (NR) was not considered. Future changes in the above-mentioned factors are hardly predictable at current conditions and whatever the Future changes either will increase or decrease the flood damages. At this end, the applied approach which assess Future damages keeping same

Present and Future conditions is deemed to be appropriate. Wobus et al. 2013 followed similar approach to estimate monetary damages due to flood in the United States. A household survey in six VDCs namely Kamdi, Banakatti, Betahini, Phatepur, Holiya, and Gangapur was carried out to assess the socioeconomic status and vulnerabilities of the local communities, and to assess the households and agricultural damage faced by the communities in the past flood events. The obtained data was then analyzed to prepare the flood–damage functions. The flood damage assessment for the floods of 50-year return periods (SPAC and SFAC) and for 2007 flood event was conducted. The flood damages for different flood conditions were assessed by combining the inundation distributions with the spatially varied damage functions derived for household and agriculture damages.

3.3.1 Household damage assessment

Households in the selected area were categorized according to their roof types as shown in Table 6. Four roof types were identified in the area: (1) cemented, (2) tile/fabric, (3) asbestos sheets, and (4) thatch/straw. It was observed during the field survey that the roofs represented the economic status of households than other household's physical characteristics such as wall type, wall thickness, or floor type. The damage curve for households, which shows the relationship between flood depth and household damages, was prepared and shown in Fig. 14. In the case of household damages, the value of household structures and domestic property values was considered. The damage calculation was based on the average damage per household and household density of the area. According to the Fig. 14, it can be noticed that with the increase in flood depth, the damage value increases and significant increment can be seen after the depth of 0.6 m. When the flood depth is above 0.9 m, cement roofed houses show high damage values compared to other roof types. The main reason is the economic status of the residence. The residence with cemented roofs was observed as high-income-level families with lots of households items such as furniture and electronic appliances, which were in high monetary values. While the other roof type households were considered as less economically strong status having only basic items for their living as domestic properties. In order to access the damage, maximum depth of inundation for the given area (grid size of 90 m × 90 m) was selected from the different

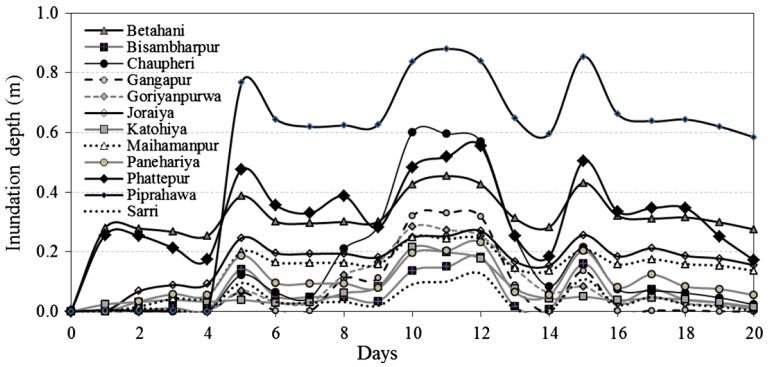

Fig. 8 Simulated inundation depths at villages for 2007 flood event. [(Holiya VDC villages: Piprahawa and Choupheri), (Gangapur VDC villages: Gangapur), (Phatterpur VDC villages: Goriyanpurwa, Joraiya, Bisabharmpur, Sarri, Mahimanpur, and Panehariya), (Bankatti VDC villages: Katohiya), (Betahani VDC villages: Betahani)]

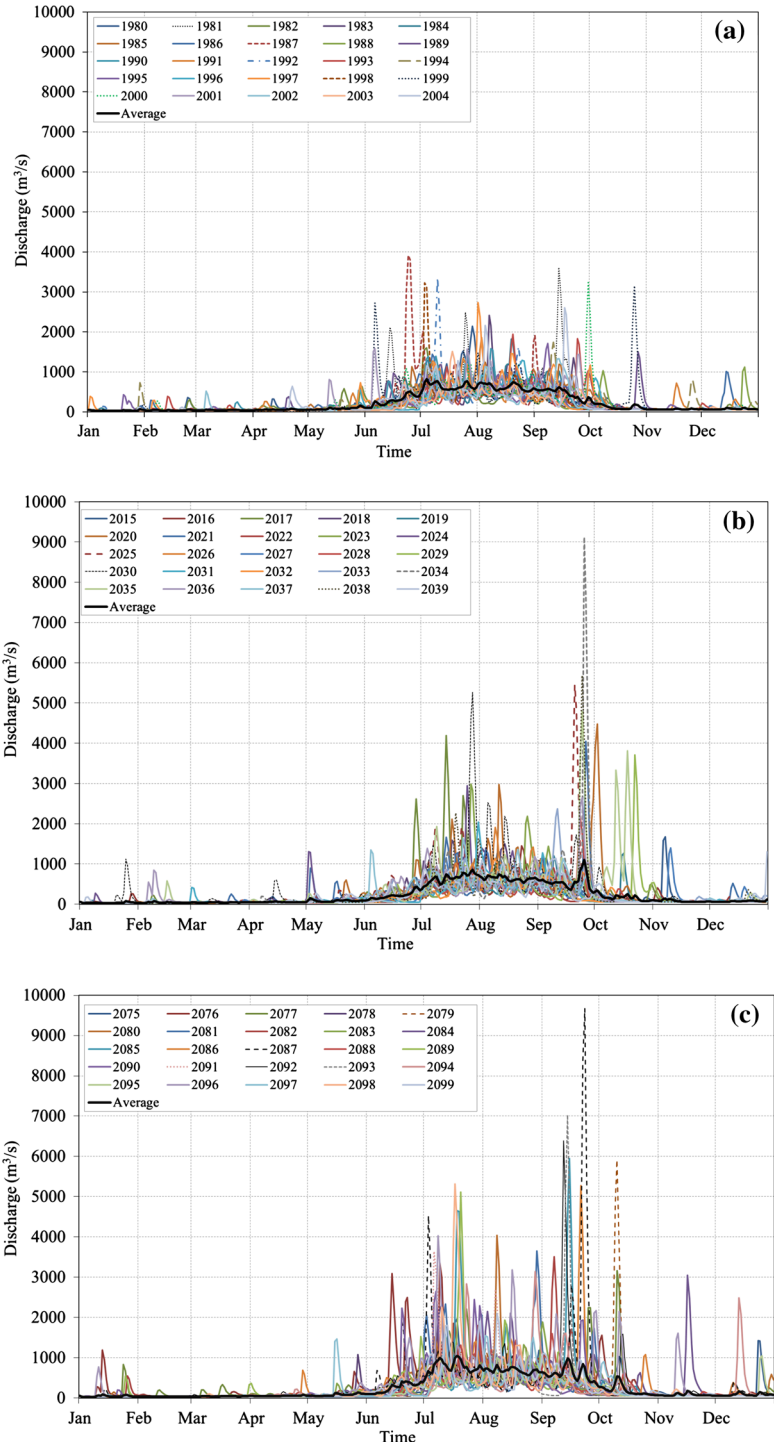

Fig. 9 Daily discharges at RRI inlet point based on MRI-AGCM 3.2 s bias-corrected precipitations. **a** SPAC, **b** SNAC, **c** SFAC

Table 10 Frequency analysis results

Threshold 1,500 m^3/s		Frequency in 25 years	Probable discharge (m^3/s)	
			25-year return period discharge	50-year return period discharge
MRI-GCM 3.1S	SPOAC	38	3,272	3,629
	SNOAC	38	4,086	4,600
	SFOAC	53	3,544	3,911
MRI-GCM 3.2S	SPAC	30	4,107	4,658
	SNAC	37	7,058	8,171
	SFAC	66	7,723	8,806
Based on observed rainfalls		43	3,906	4,354

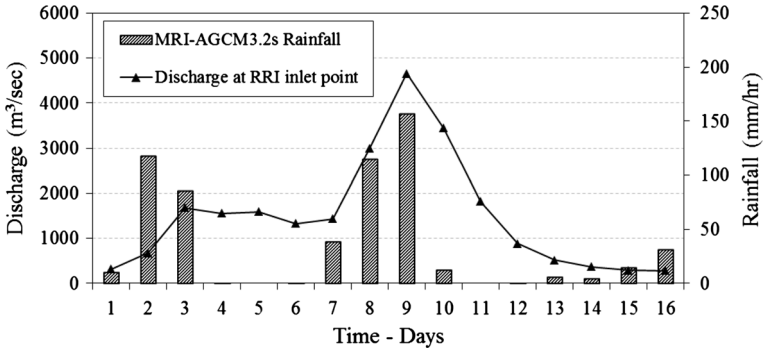

Fig. 10 SPAC 50-year return period RRI inlet discharge hydrograph and rainfall

depths in different duration (in days) of simulation. As such, maximum flood depth raster was created. The household density map of 2011 was prepared based on the projected population of 2011 from the 2001 census using the annual growth rate of Banke District where the study area was located. The settlement areas were selected from land-cover map and converted into the raster of 30 m × 30 m. The raster size of 90 m × 90 m was the resolution where inundation simulation carried out was not used directly because it would not clearly delineate the settlement areas. Therefore, smaller cell size (30 m × 30 m) was created for the settlement. For the analysis, to make cell size uniform, the maximum flood depth raster was resampled by using "nearest neighbor" technique from 90 m × 90 m to 30 m × 30 m. Once the raster was created, for the cells where there were settlements, the re-sampled maximum depth raster was reclassified into damage value (NRs per household) using the damage curve shown in Fig. 14. The special distribution of household flood damages for 2007 flood is depicted in Fig. 15. Household damage assessment was conducted for the villages shown in Fig. 7 of each VDCs. Since the topography of the area is plain and the houses' floor levels are not raised above the ground level, even in a small flood event, those houses get inundated. Household damage comparison was conducted based on the 2007 event, and it is shown in Fig. 16. The gradual increment of damages can be noticed for all the VDCs when shifting from 2007 flood to 50-year return period floods

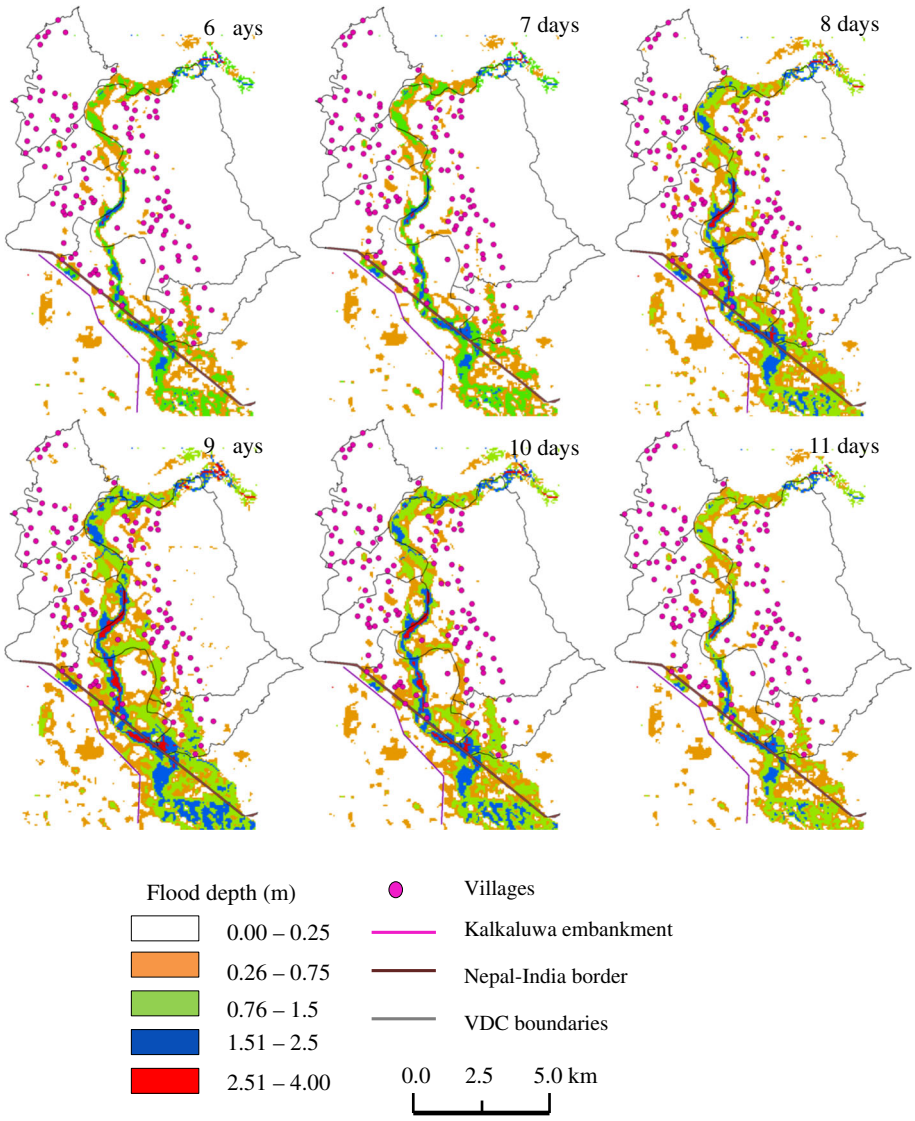

Fig. 11 SPAC 50-year return period inundation based on Fig. 10 rainfall and discharge

of SPAC and SFAC. The highest damage value was calculated for Phattapur VDC for all types of flood events. The highest household damage is above 125 million of Nepal Rupees obtained for Phattapur, which covers large land area compared to other VDCs. However, the damage increment ratio is concerned for SPAC and SFAC, and Holiya can be ranked as the severely affected VDC. It shows 2.84 and 4.53 increment ratios for SPAC and SFAC, respectively. According to the field survey observations, Holiya was categorized as most affected VDC, and in Future also, Holiya will remain as a most affected VDC. Gangapur, the other most affected VDC, shows second highest increment ratios after Holiya for SPAC

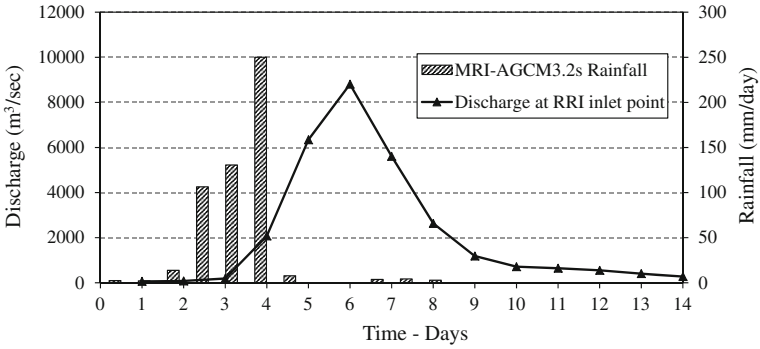

Fig. 12 SFAC 50-year return period RRI inlet discharge hydrograph and rainfall

and SFAC 50-year return period floods. Kamdi, which is located in the upstream of the study area, shows lowest damage increment ratio.

3.3.2 Agricultural damage assessment

Damages caused to paddy by floods were considered in the agricultural damage assessment since paddy was the main crop in the selected area. In Nepal, in 2009/10, the highest yield of paddy was in Bara District with the value of 3.5 Mt/ha (MOAD 2012). This value was used as the yield value in Future (SFAC) paddy yield. The paddy yield in the area (as of Banke District 2009/10) 2.96 Mt/ha (MOAD 2012) was used for SPAC. Figure 17 explains the paddy yield over the time period of 1993/94 to 2009/10. The average yield in the area was calculated as 2.96 Mt/ha. The Present price of the paddy is NRs. 15,000 per Mt (Field Survey, 2011). Damage to the paddy was determined by two factors: flood depth and duration. The data collected during the field survey for the paddy damages for past flood events were analyzed, and paddy damage curve was prepared and it is shown in Fig. 18. Agricultural damage for different flood conditions was calculated based on the different flood depths for different duration obtained from the simulation results. The core of the calculation based on the agricultural damage function was prepared for paddy from the field survey 2011. From the field study, the thresholds depth delineating the damage values was 30, 20, and 10 cm. According to the damage function of paddy obtained from field survey, for the depth above threshold of 20 cm, the damage for more than 3 days of inundation would lead to 100 % damage of crops while the damage percent would be 75 % for the inundation duration between 2 and 3 days. Likewise, the damage percent would be 50 % for the inundation duration of 2 days. The paddy often cultivated in the area has a characteristic of less height than usual paddy, and the damage values obtained during the field survey were mainly for the growing stage of rice plants. Tables 13 and 14 summarize the loss and total damages of paddy during the flood season as of the field survey data. For the different threshold conditions of depths of inundation, there were different damage values (percentages). Then, the value of the damage (percentage) was multiplied by the monetary value of the crop for the corresponding location (cell) to yield the damage amount. Among those values, the maximum value for the given location was taken as the damage value for the analysis. The steps are listed in brief as follows:

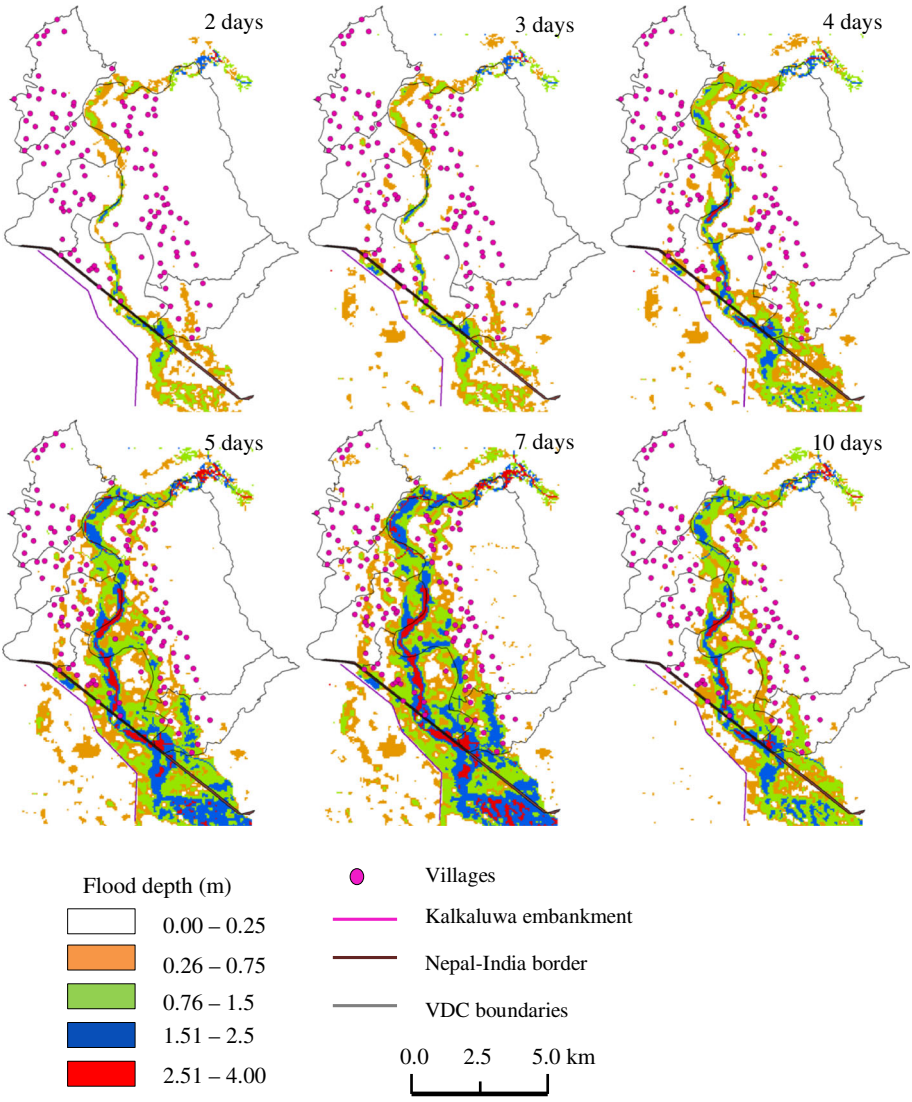

Fig. 13 SFAC 50-year return period inundation based on Fig. 12 rainfall and discharge

Table 11 Inundation area where the flood depths equal or exceed 30 cm at the flood peak compared to 2007 flood

2007 flood, A_{2007} (km^2)	SPAC flood, A_{SPAC} (km^2)	SFAC flood, A_{SFAC} (km^2)	Increment $\frac{A_{SPAC}}{A_{2007}}$	Increment $\frac{A_{SPAC}}{A_{2007}}$
60	106	133	1.8	2.2

Table 12 Summary of inundation analysis for SPAC and SFAC

	SPAC: (1980–2004)	SFAC: (2075–2099)	Increment ratio
1/50 precipitation (daily basin average mm/day)	139	212	1.53
Frequency of precipitation exceeding 50 mm/day	57	105	1.84
1/50 peak discharge (m^3/s)	4,660	8,810	1.89
Frequency of discharges exceeding 1,500 m^3/s	30	66	2.20
Inundation area where the flood depth is more than 30 cm (km^2)	106	133	1.25

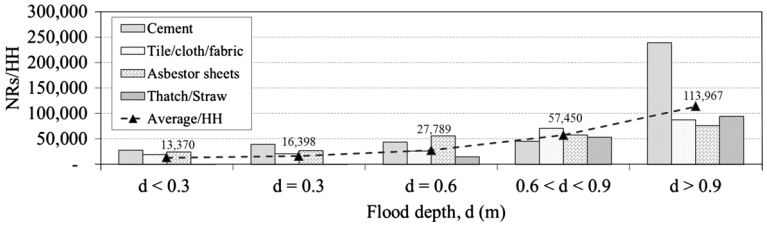

Fig. 14 Household damage curve

a. For a location (cell), read the depths of inundation for total number of flood simulation days
b. Set the first threshold depth, for, e.g., 30 cm
c. Identify the number of peak over threshold depth with the corresponding number of subsequent days of inundation
d. Choose the peak over threshold with the maximum duration of inundation
e. Assign the damage value for the selected condition according to damage curve
f. Store this damage value
g. Repeat the steps form (b) to (f) for different threshold depths
h. Choose the maximum damage value from the sets of damage value for different threshold depths
i. Multiply the damage value with the monetary crop value of the location (cell) under consideration. This yields the agricultural damage value for given cell
j. Carry out all the above steps for all cells in the entire study area.

Following above steps, monetary value raster for agriculture damages was prepared. The agricultural productivity of the area was 2.96 Mt/ha, and for each grid (90 m × 90 m), the production value was 2.4 Mt for SPAC case, for the SFAC, the productivity was 3.5 Mt/ha, and for each grid, it was 2.83 Mt. The monetary value of 1 Mt of paddy was NRs 15,000. Therefore, each grid represents the value of NRs 36,000 for SPAC and NRs 42,450 for SFAC of paddy where the land use was represented by paddy. The calculated agricultural damage for 2007 and 50-year return period floods of SPAC and SFAC is shown in Fig. 19.

In agriculture damages, Phattapur and Holiya show highest ratios compared to other VDCs, although in monetary values, Kamdi has lowest damages compared to other 5 VDCs according to Fig. 20. Holiya which has high damage increment ratios in household damages, shows significantly high damage increment ratios in agriculture damages as well.

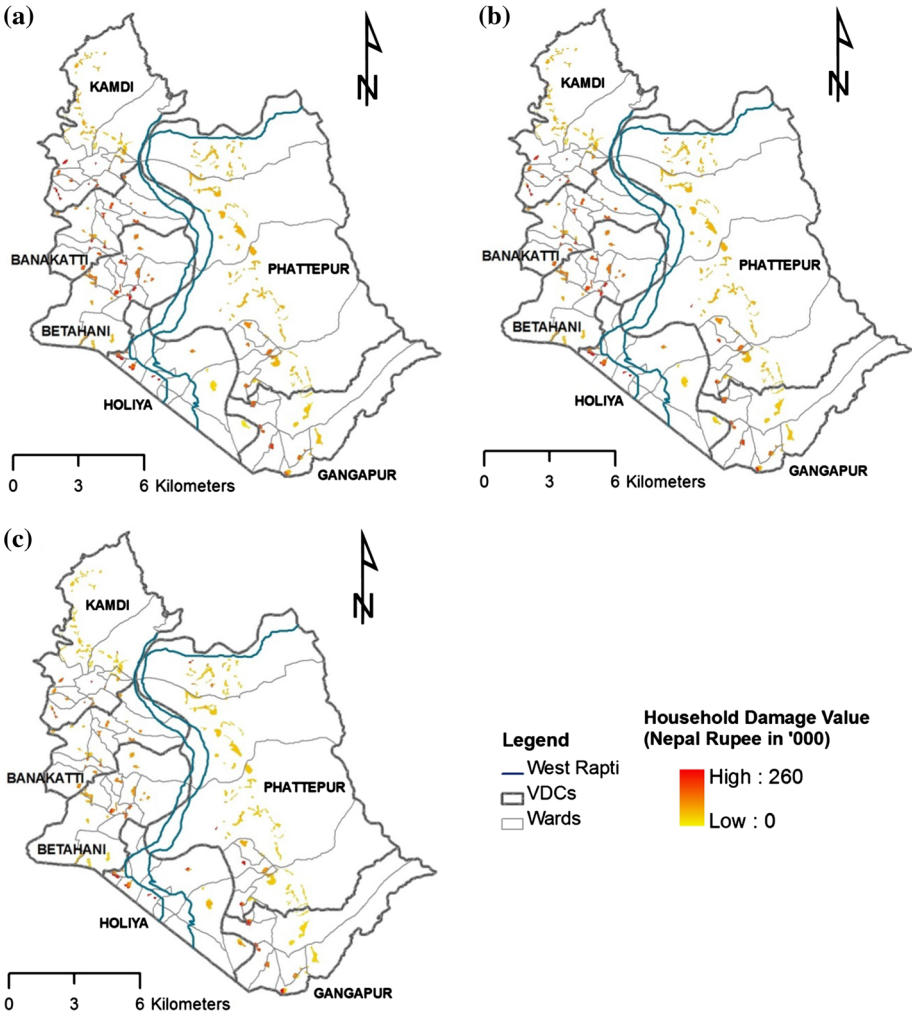

Fig. 15 Household damage distribution at VDCs for **a** 2007 flood event, **b** SPAC 50-year return period flood event, **c** SFAC 50-year return period flood event

Holiya, Gangapur, and Betahani VDCs, which have boundaries to the Nepal–India border, show relatively high damage increments from 2007 flood to 50-year return period floods of SPAC and SFAC. The total agricultural damage for SPAC and SFAC 50-year return period floods was estimated as 141 and 164 million of Nepal Rupees. Even though the total agriculture damage of the area is lower than that of household damages, the impact is relatively high since agriculture is the main income of the local communities of the area.

4 Conclusion

This study discussed an approach to estimate household and agricultural damages due to flooding under climate change utilizing high-resolution MRI-AGCM outputs. This

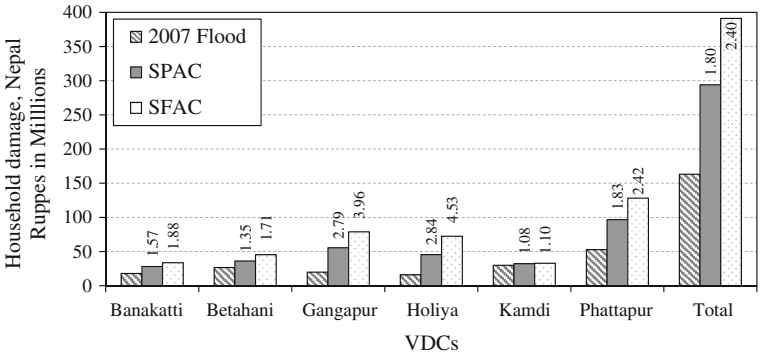

Fig. 16 Household damage comparison for 2007, SPAC, and AFAC flood events. Increment ratios compared to 2007 damages area also shown for each VDC

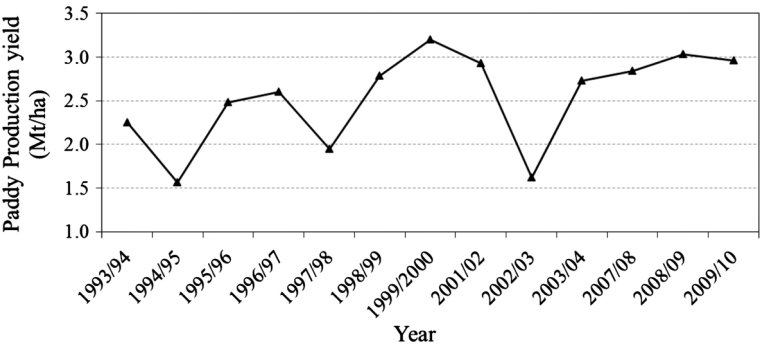

Fig. 17 Paddy yield variation over time 1993/94–2009/10

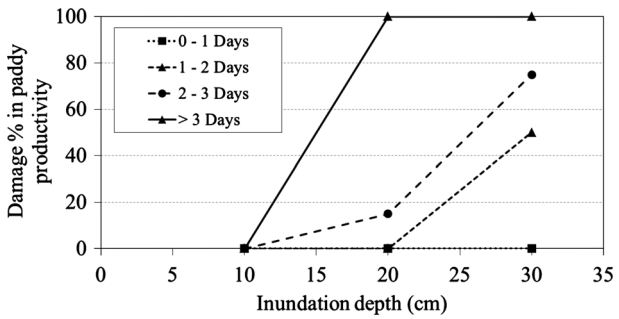

Fig. 18 Damage percentage of paddy production under different flooding conditions (according to the field survey data)

approach can be applied to estimate flood damages in broader aspect to evaluate anticipated climate change in future due to greenhouse gas emission. Due to the localized scale of this analysis, we were able to apply two hydrological models to generate river runoff

Table 13 Loss in paddy yield (Mt/ha) in various flooding conditions

Duration/depth	Loss in paddy yield (Mt/ha) in various flooding conditions		
	10 cm	20 cm	30 cm
0–1 days	0.00	0.00	0.00
1–2 days	0.00	0.00	1.48
2–3 days	0.00	0.44	2.22
>3 days	0.00	2.96	2.96

Table 14 Total damage in monetary terms (NRs./ha) for various flooding conditions

Duration/depth	Total damage in monetary terms (NRs./ha) due to various flooding conditions		
	10 cm	20 cm	30 cm
0–1 days	0	0	0.00
1–2 days	0	0	222,000
2–3 days	0	6,660	333,000
>3 days	0	444,000	444,000

NRs Nepal Rupees

and flood inundation. While this approach provides a local-scale method to estimate flood damages, still the limitations and uncertainties are to be addressed in further studies.

Integrated approach of social and hydrological sciences has introduced to analyze the socioeconomic impacts of anticipated floods. Coupling of MRI-AGCM precipitations with hydrological models and social survey data was employed in the lower WRR basin to examine the potential impacts of climate change on flood hazards and consequent flood damages. Although AGCM 3.1S and 3.2S were used to show differences in future projections, we mainly focused on the 3.2S output-based results since it gave the most extreme conditions. High-resolution MRI-AGCM outputs application was significantly effective in the approach, which provides stage for the direct application of AGCM outputs after correcting bias without downscaling. The usual practice of employing either scenario-based or risk-based approaches to investigate potential implications of climate change was not applied in this study. Instead of that, we focused on return period floods based on Present, Near-Future, and Future river runoffs. The obtained 50-year return period river discharges for Present and Future time series were 4,658 and 8,806 m^3/s, respectively. We have employed a systematic approach for utilize high-resolution AGCM outputs to investigate future flood hazards of lower WRR basin where so far none of research has carried out. Bias-corrected precipitation data were applied to PDHM to simulate river runoff. It showed that the annual average rainfall in Future was intensive than Present and Near-Future. The river discharges also show similar pattern accordingly. Extremely high 50-year return period floods were resulted in the frequency analysis, and the inundation simulations were carried out based on those runoff values. Flood occurred in 2007 was also simulated, and 50-year return period floods' damages were estimated and increment ratios based on 2007 flood event was calculated. The inundation and damage distributions at that extreme flood event suggests that in Future, the VDCs which were grouped as most

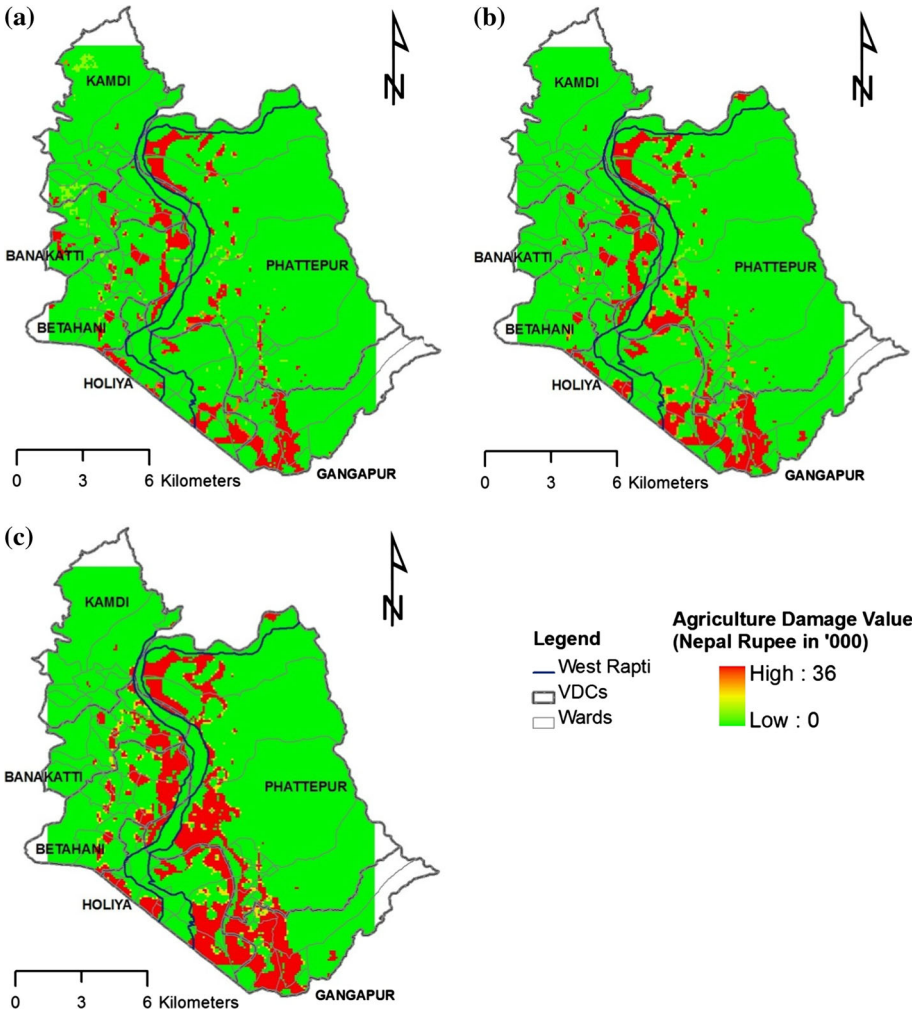

Fig. 19 Agricultural damage distribution at VDCs for **a** 2007 flood event, **b** SPAC 50-year return period flood event, **c** SFAC 50-year return period flood event

effected will be severely affected unless proper structural and non-structural counter measures are established. The potential agricultural damages in Future will cause high economic damages that ultimately can lead to social catastrophes also. As our final goal of simulate floods for Present and Future anticipated extreme events and assess the household and agricultural damages, the goal has been achieved. In this study, we used only MRI-AGCM outputs with one rainfall pattern for each 50-year return period; however, it is recommended to use other GCM outputs also to find out the impact of climate change with several rainfall patterns. The approach developed in this study is applicable to any other basin also to understand future flood hazards.

The authors believe that the flood risk assessment based on a combination of potential flood hazed due to climate change, vulnerability, and exposure presented in the paper

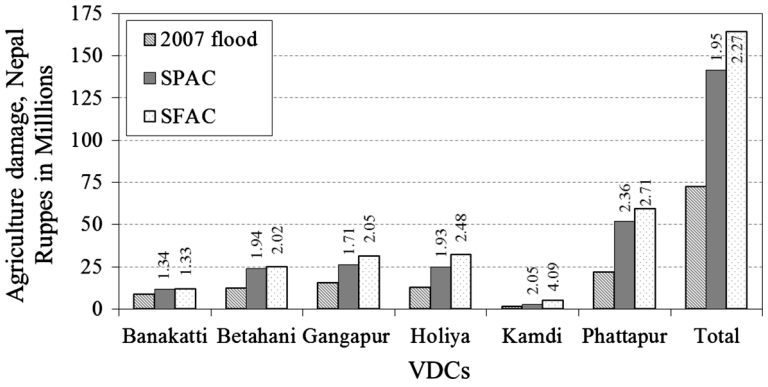

Fig. 20 Agricultural damage comparison for 2007, SPAC, and SFAC flood events. Increment ratios compared to 2007 damages area also shown for each VDC

provides the baseline information of the current situation in the study area without the influence of the proposed infrastructure (e.g., Naumure project) or the structures exist outside the study area such as Laxmanpur barrage and Sikta irrigation project. However, the methodology and work presented in this paper can be beneficially used to assess the benefits of such flood regulation structures by comparing the flood damages with or without the infrastructures. Impact of any future infrastructure can then be compared with the baseline situation to derived the benefits and implications to flood risk in the area. Use of community level survey to derive the vulnerability (damage curve) is an important part of the flood risk assessment. These damage curves showed that household and agriculture depended on depth, duration, location, and time of flood water. Vulnerable population and assets were mapped and combined with damage and hazards conditions to derive total flood damages.

The factors which were not considered in the present study such as bank-cutting, erosion, and sedimentation will never minimize the results of the study but possibly make the flood disaster even worse. Besides, the study did not consider the future river bank development activities. Therefore, the present results would be a scenario that discusses the situation if no flood protection action taken place in future. In this context, the results of present study have a significant meaning by itself as the first step to understand the increase in flood risk due to climate change, in spite of neglecting the effects of bank-cutting, erosion, and sedimentation. The authors also understand the uncertainty of the climate change prediction by MRI-AGCM. We regarded the MRI-AGCM outputs as one of the newest and most sophisticated AGCMs in the world with very fine special resolution. The uncertainty of the future climate prediction is still a hottest topic of discussion even in advanced meteorology and climatology. Understanding of such uncertainties should be also the next step of the study. More sophisticated studies should be carried out to understand the future more clearly in the sense of flood hazards, damages, and risk assessments overcoming uncertainties. The integrated approach of hydrological modeling and socioeconomic study enabled to elaborate the future flood hazards under limitations as explained in previous sections and appeal for further investigations in long-term flood disaster mitigation and community-based adaptation programs for the lower WRR basin.

Acknowledgments This work was conducted under the framework of the "assessment of the impact of climate change on flood disaster risk and its reduction measures over the globe and specific vulnerable areas" of Japan supported by the Innovative Program of Climate Change Projection for the 21st Century (KAKUSHIN) of the Ministry of Education, Culture, Sports, Science, and Technology (MEXT), Japan. Expertise support for inundation modeling given by Dr. Takahiro Sayama at ICHARM is gratefully acknowledged by the authors.

References

Baidya SK, Regmi RK, Shrestha ML (2007) Climate profile and observed climate change and climate variability in Nepal. Department of Hydrology and Meteorology Kathmandu, Nepal

Brouwer R, van EkR (2004) Integrated ecological, economic and social impact assessment of alternative flood control policies in the Netherlands. Ecol Econ 50:1–21

Central Bureau of Statistics (2001) Statistical year book of Nepal. National Planning Secretariat, Nepal

Chen H, Xiang T, Zhou X, Xu C (2012) Impact of climate change on the Qingjiang Watershed's Runoff Change Trend in China. Stoch Env Res Risk Assess 26(4):847–858

Chow VT, Maidment DR, Mays LW (1988) Applied hydrology. McGraw-Hill, New York

Department of Irrigation, Nepal (2014) Sikta irrigation project. http://www.doi.gov.np/projects/project.php?pid=19. Accessed 20 Jan 2014

Department of Water Induced Disaster Prevention (2004) Disaster reviews from 1983–2004. Lalitpur, Nepal

Department of Water Induced Disaster Prevention (2007) Disaster review 2006, Series XIV, Kathmandu, Nepal

Dilley M, Chen RS, Deichmann U, Lerner-Lam AL, Arnold M (2005) Natural disaster hotspots: a global risk analysis. The World Bank Group, Washington

Dutta D, Tingsanchali T (2003) Development of flood loss functions for urban flood risk analysis in Bangkok. In: Proceedings of the 2nd international conference on new technologies for urban safety in mega cities of Asia, 30–31 October, University of Tokyo, Japan, pp 229–238

Food and Agriculture Organization (2004) Compendium of food and agriculture indicators 2004—Nepal. www.fao.org/es/ess/compendium_2004/pdf/ESS_NEP.pdf

Gautam DK, Phaiju AG (2013) Community based approach to flood early warning in West Rapti River basin of Nepal. J Integr Disaster Risk Manage 3(I):1–11. doi:10.5595/idrim.2013.0061

Inomata H, Fukami K (2007) Development of a system for estimating flood risk in the Yoshino river basin. J Adv River Eng 13:433–438

Inomata H, Takeuchi K, Fukami K (2009) Development of a statistical bias correction method for daily precipitation data of GCM20. Annu J Hydraul Eng 55:247–252

IPCC (2007) Summary for policymakers. In: Solomon S, Qin D, Manning M, Chen Z, Marquis M, Averyt KB, Tignor M, Miller HL (eds) Climate change 2007: the physical science basis. Contribution of working group I to the fourth assessment report of the Intergovernmental Panel on Climate Change. Cambridge University Press, Cambridge

Jonge TD, Matthijs K, Hogeweg M (1996) Modeling floods and damage assessment using GIS. In: Kovar K, Nachtnebel HP (eds) Application of geographic information systems in hydrology and water resource management. Proceedings of HydroGIS 96. IAHS Press, IAHS Publ, Wallingford 235:299–306

Jonkman SN et al (2008) Integrated hydrodynamic and economic modelling of flood damage in the Netherlands. Ecol Econ 66:77–90

Kamiguchi K, Arakawa A, Kitoh A, Yatagai A, Hamada A, Yasutomi N (2010) Development of APHRO JP, the first Japanese high-resolution daily precipitation product for more than 100 years. Hydrol Res Lett 4:60–64. doi:10.3178/HRL.4.60

Kitoh A, Ose T, Kurihara K, Kusunoki S, Sugi M (2009) Projection of changes in future weather extremes using super-high-resolution global and regional atmospheric models in the KAKUSHIN program: results of preliminary experiments. Hydrol Res Lett 3:49–53

Lehner B, Verdin K, Jarvis A (2008) New global hydrography derived from space borne elevation data. EOS Trans AGU 89:93–94

Ministry of Agriculture and Development-Nepal (2012) Statistical information on Nepalese agriculture 2011/2012. Kathmandu, Nepal

Ministry of Finance-Nepal (2005) Economic survey—fiscal year 2004/05. Kathmandu, Nepal

Mizuta R, Yoshimura H et al (2012) Climate simulations using MRI-AGCM 3.2 with 20-km grid. J Meteorol Soc Jpn 90A:232–258

Nicholls RJ (2002) Analysis of global impacts of sea-level rise: a case study of flooding. Phys Chem Earth 27:1455–1466
Nicholls RJ, Hoozemans FMJ, Marchand M (1999) Increasing flood risk and wetland losses due to global sea level rise: regional and global analyses. Global Environ Change 9:S69–S87
Osti R (2008) A feasibility study on integrated community based flood disaster management of Banke district, Nepal Phase 1(a): baseline study. Technical note of PWRI No. 4122, Tsukuba, Japan
Parker DJ (1992) The assessment of the economic and social impacts of natural hazards. International conference on Preparedness and Mitigation for Natural Disasters, 28–29 May, Reykjavik, Iceland
Parry M, Arnell N, McMichael T et al (2001) Millions at risk: defining critical climate change threats and targets. Glob Environ Change 11(III):181–183
Sayama T, Ozawa G, Kawakami T, Nabesaka S, Fukami K (2011) Rainfall-runoff-inundation analysis of Pakistan flood-2010 at the Kabul river basin. Hydrol Sci J 57(II):298–312
Sugiura T, Fukami K et al (2009) Development of an integrated flood analysis system (IFAS) and its applications. In: 7th ISE and 8th HIC, Chile
United Nations Development Program (2009) Nepal disaster report. Government of Nepal, Ministry of home affairs and Nepal disaster preparedness network Nepal
United Nations Office for the Coordination of Humanitarian Affairs (2009) Nepal FWR/MWR floods and landslides, Situation report #2
Vaze J, Teng J (2011) Future climate and runoff projections across New South Wales, Australia: results and practical applications. Hydrol Pros 25:18–35. doi:10.1002/hyp.7812
Wobus C, Lawson M, Jones R, Smith J, Martinich J (2013) Estimating monetary damages from flooding in the United States under changing climate. J Flood Risk Mangt. doi:10.1111/jfr3.12043
Yatagai A, Arakawa O, Kamiguchi K, Kawamoto H, Nodzu M, Hamada A (2009) A 44-year daily precipitation dataset for Asia based on a dense network of rain gauge. SOLA 5:137–140. doi:10.2151/sola.2009-035